High-frequency waves guided by the subducted plates underneath Taiwan and their association with seismic intensity anomalies

Kate Huihsuan Chen,[1] Brian L. N. Kennett,[2] and Takashi Furumura[3]

[1]   Energy from seismic events traveling up a subduction zone is frequently associated with significant large-amplitude, high-frequency signals with sustained long coda. Such seismic waves guided by the subducted plate with high wave velocity and high Q can cause surprisingly large seismic intensity in the fore-arc area. In this study, we characterize the guiding behavior of the subducted Philippine Sea plate (PSP) underneath Taiwan and investigate their relationship with anomalous peak ground acceleration (PGA) patterns. Oblique subduction of Philippine Sea Plate beneath northeast Taiwan complicates the guiding phenomena. Seismic waves from events deeper than 60 km offshore northern Taiwan reveal wave guide behavior: large, sustained high-frequency (3–10 Hz) signal in P and S wave trains. With increasing depth, a low-frequency (<1 Hz) first arrival becomes more significant especially for events deeper than 100 km. The time separation between the low-frequency onset and the later high-frequency arrival slightly increases with depth, while the value varies with station due to different travel distances in the shallow crust. The depth-dependent high-frequency content confirms the association with a waveguide effect in the subducting slab rather than localized site amplification effects. We attempt here to obtain a practicable quantification scheme to determine the duration of higher-frequency energy, which can be regarded as an indicator of the guiding effect of the Philippine Sea Plate.

1.   Introduction

[2]   The large velocity gradient and stochastic variations in a subducting slab act as a waveguide to transmit high-frequency energy efficiently to the surface. The seismic signals with longest interaction times propagating inside the slab exhibit (1) very large high frequency signals, (2) distortion in P and S wave pulse shapes and long coda, and (3) different first arrivals for long- and short-period energy; such effects have been reported worldwide. A low-frequency first arrival followed by large-amplitude, high-frequency signals with sustained coda are often found at stations in the fore-arc side of the subduction zone from intermediate-depth earthquakes [e.g., *Utsu*, 1966; *Abers*, 2000; *Abers et al.*, 2003; *Martin et al.*, 2003; *Furumura and Kennett*, 2005; *Furumura and Kennett*, 2008], and high-frequency first arrival followed by

low-frequency later signal is also observed in other subduction zones such as Tonga and New Zealand [e.g., *Ansell and Gubbins*, 1986; *van der Hilst and Snieder*, 1996]. A plate model with high-seismic speed (high-V), low-attenuation (high-Q) structure, and a large contrast to the surrounding low-V, low-Q mantle explains the amplified high-frequency signals [*Utsu*, 1966]. However, such a simple model cannot explain the long-lasting high-frequency coda. A thin, low-V zone of former oceanic crust at the top of the plate can also act as an efficient waveguide [*Abers*, 2000; *Abers et al.*, 2003; *Martin et al.*, 2003; *Martin and Rietbrock*, 2006]; however, such low-V layer is unlikely to survive below a depth of 100 km where the transformation to high-velocity ecologite is taking place [*Kita et al.*, 2006; *Kawakatsu and Watada*, 2007; *Tsuji et al.*, 2008] and so fails to explain the guided waves from events deeper than 200 km in Japan (indeed down to 600 km depth). An alternative model proposed by *Furumura and Kennett* [2005] suggests that the small-scale heterogeneity characterized by velocity fluctuation in the subducting plate plays an important role. In their model, the multiple forward scattering of high-frequency waves within the plate produces high-frequency guided behavior. Using 2-D and 3-D finite-difference method wave propagation simulation, *Furumura and Kennett* [2005] argue that the elongated shape of heterogeneity within the plate with much longer correlation along-strike distances is capable of producing long duration of high-frequency energy.

All Supporting Information may be found in the online version of this article.
[1]Department of Earth Sciences, National Taiwan Normal University, Taipei, Taiwan.
[2]Research School of Earth Sciences, The Australian National University, Canberra, ACT, Australia.
[3]Earthquake Research Institute, University of Tokyo, Tokyo, Japan.

Corresponding author: K. H. Chen, Department of Earth Sciences, National Taiwan Normal University, No.88, Sec. 4, Tingzhou Rd., Wenshan District, Taipei 11677, Taiwan. (katepili@gmail.com)

[3] Such seismic waves guided by the high wave velocity and high Q, descending plate are found to cause surprisingly large intensity in the fore-arc area of Japan, even if the events are not felt near the epicenter [*Utsu*, 1966; *Fukao et al.*, 1983]. The abnormal intensities in Japan have been well recognized since the early 1900's [e.g., *Hasegawa*, 1918; *Ishikawa*, 1926] and linked to the presence of high-frequency signals guided within the subducted plate [*Utsu*, 1966; *Utsu and Okada*, 1968; *Fukao et al.*, 1983; *Chiu et al.*, 1985; *Furumura and Kennett*, 2005; *Furumura and Kennett*, 2008]. For fore-arc stations where large intensity is concentrated, the broadband seismograms reveal tens to a few hundred times greater amplitude than a comparable back-arc station in the higher-frequency range from 4 to 20 Hz (e.g., the PSP event in Figure 5 in *Furumura and Kennett* [2008]). The amplified, sustained high-frequency signals due to traveling through the heterogeneous plate referred to as plate guiding events are, therefore, responsible for the abnormal distribution of ground shaking.

[4] Taiwan, situated at the complicated plate boundary zone between the Eurasian plate (EP) and the Philippine Sea Plates (PSPs), exhibits a unique interaction between the EP and PSP. In northeast Taiwan, the PSP subducts beneath the rifted Eurasian plate margin along the Ryukyu Trench at a rate of 8 cm/yr to the north-west [*Seno*, 1977; *Seno et al.*, 1993; *Yu et al.*, 1977], whereas in southwest Taiwan, the Eurasian plate subducts underneath PSP along the Malina trench (Figure 1). The active mountain belt in Taiwan is therefore a result of collisions between the Luzon arc and the Asian continent [*Biq*, 1973; *Bowin et al.*, 1978; *Ho*, 1986]. There has been a considerable debate about how the eastward dipping EP and the northward dipping PSP meet underneath Taiwan. The exact plate boundary is difficult to define precisely because of the absence of deep earthquakes in Central Taiwan (north of 23°N) and the limitations of the tomographic models due to one-sided station coverage as a consequence of seaward subduction. While the present-day plate configuration derived from different seismological data/method [e.g., *Wu et al.*, 1997; *Kao et al.*, 1998; *Chou et al.*, 2006; *Wu et al.*, 2007; *Wu et al.*, 2009; *Ustaszewski et al.*, 2012] suggests slightly different PSP termination boundaries against eastern Taiwan [*Wu et al.*, 2009, Figure 1], the presence and continuity of the EP underneath Central Taiwan is still controversial [*Lin*, 2002; *Chen et al.*, 2004; *Wang et al.*, 2006; *Lin*, 2009; *Wang et al.*, 2009].

[5] If the subducting PSP in the north and EP in the south acts as a waveguide for high-frequency seismic waves, the observation of slab-guided waves may provide independent constraint on slab continuity. Most importantly, slab-induced anomalous seismic intensity from intermediate-depth earthquakes could happen in Taiwan, with consequence for assessment of seismic hazard. However, the characteristics of guided
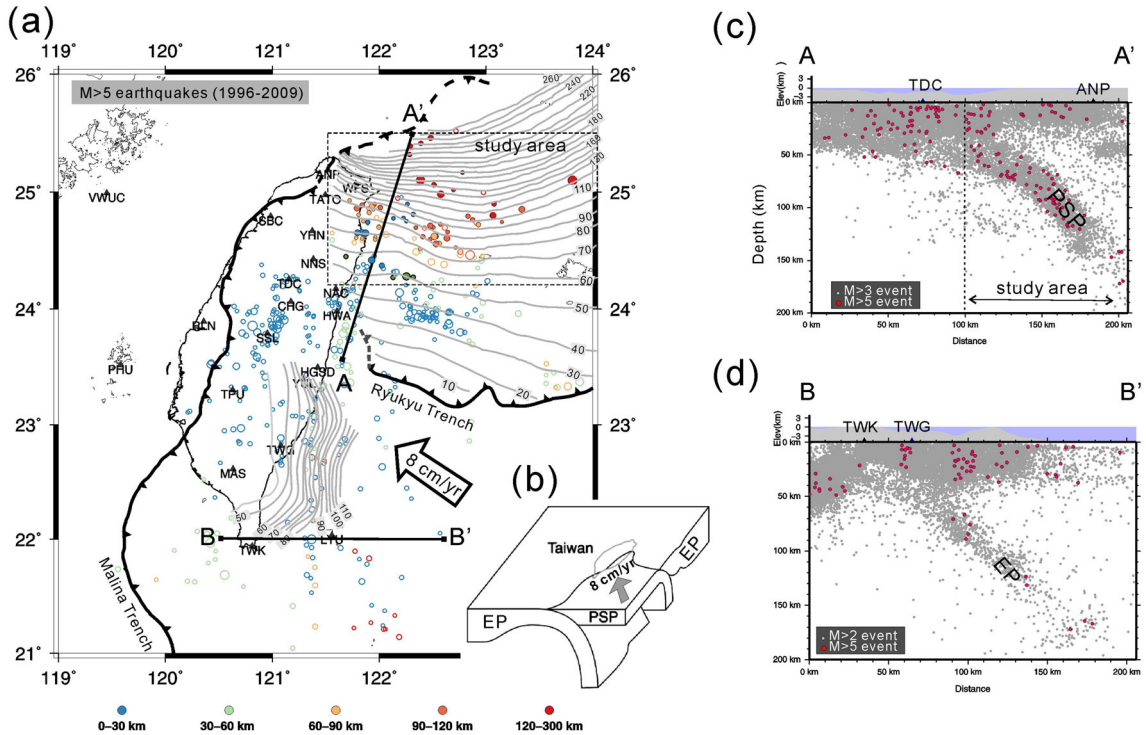

Figure 1. (a) The distribution of BATS broadband stations (black triangles) and M ≧ 5 earthquakes from 1996 to 2009, color coded by focal depth. Earthquakes in the spatial range of latitude 24.2°–25.5°N and longitude 121.5°–124.0°E are selected in this study (dashed box). Filled circles represent the selected events with waveforms recorded at more than five stations. Gray contours indicate the iso-depth of the PSP and EP Moho [*Ustaszewski et al.*, 2012]. (b) Simple 3-D perspective view of plate interaction beneath Taiwan [*Lallemand et al.*, 2001]. (c) Cross sections showing background seismicity (1991–2009) along profiles A-A′ and B-B′, indicating the configuration of the subducted Philippine Sea Plate (PSP) on profile A-A′ and the Eurasian plate (EP) on profile B-B′. Red circles indicate the $M \geqq 5$ events. Gray circles in Figures 1c and 1d represent $M \geqq 3$ and $M \geqq 2$ events, respectively.

waves in Taiwan subduction zones and the conditions for which the guiding effect would cause anomalous seismic intensity are still poorly known. In the present paper, we aim to demonstrate the nature of waveforms and frequency content and peak ground acceleration (PGA) patterns for plate guiding events, and to explore the relation between the characteristics of the guided waves and seismic intensity anomalies. We also provide additional information for the plate configuration and continuity of subducted materials underneath Taiwan.

2. Anomalous PGA Pattern Due To Guided Wave Along Philippine Sea Plate From Deep Focus Earthquake

[6] A recent deep focus M6.8 (8 Nov. 2011) earthquake near Okinawa reveals anomalous seismic intensity patterns in both Taiwan and Japan. This event occurred in the Eastern China Sea in the PSP at depth of 230 km. Figure 2a illustrates the distribution of horizontal PGA in western Japan and Taiwan from the combined data of the dense K-NET and KiK-net strong motion networks in Japan and strong motion and broadband seismic networks (Central Weather Bureau Seismic Network, CWBSN, and Broadband Array in Taiwan for Seismology, BATS) in Taiwan. Seismic intensity is observed in the range of 0.2–61.8 cm/s^2 on the nearby Ryukyu islands, with maximum acceleration of 61.78 cm/s^2 in Okinawa located ~200 km from the epicenter. North of Ryukyu islands to Kyushu, the intensity is still as large as 9.2 cm/s^2 near Kagoshima, which is 650 km away from the epicenter (Figure 2b). Here the maximum acceleration is determined from the combination of the EW and NS components of the seismogram. There is a large contrast of PGA across the volcanic front in Kyushu with anomalous extension of PGA contours along the iso-depth contour as shown in Figure 2b. For a similar epicentral distance, acceleration greater than 3 cm/s^2 occurred on the eastern coast of Kyushu (fore-arc side), whereas in western Kyushu (back-arc side), the acceleration is much smaller (<2 cm/s^2). Comparison of the acceleration waveform from a KiK-net surface station at the fore-arc side (KGSH12) and the back-arc side (KGSH03) also illustrates a pronounced difference in amplitude and frequency content. As shown in Figure 2d, a high-frequency signal in the range 5–10 Hz is dominant in both P and S waves at KGSH12, whereas at KGSH03, high-frequency signals are attenuated.
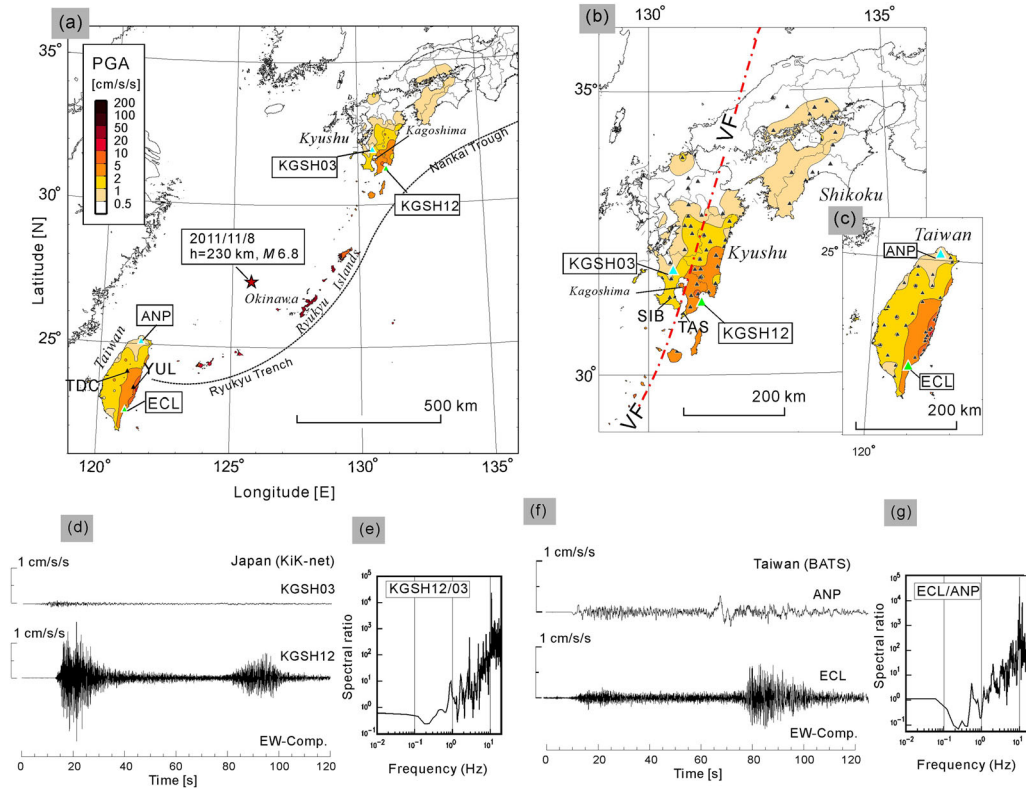

Figure 2. (a) Map of distribution of horizontal peak ground acceleration (PGA) across Taiwan and Japan for a deep focus M6.8 earthquake behind the Ryukyu trench on 8 November 2011 at a depth of 230 km. The PGA values in Japan are derived from K-NET and KiK-net strong motion networks, whereas the values in Taiwan are from strong motion and broadband (BATS and CWBSN) networks. (b) and (c) show close-up views of the PGA map in Japan and Taiwan. The gray dashed line denotes iso-depth contours of the subducting Philippine Sea Plate beneath Ryukyu trench, and red dashed line denotes volcanic front. (d and f) Examples of EW-component ground acceleration seismograms (120 s) and spectra (10 s window from 0.5 s before P arrival) at fore-arc side and back-arc side of the volcanic front in Kyushu (KGSH12 and KGSH03) and in Taiwan (ECL and ANP), respectively. (e and g) Comparison of spectral ratio of broadband waveforms at fore-arc side and back-arc side of the volcanic front in Kyushu (KGSH12 and KGSH03) and in Taiwan (ECL and ANP).

[7] Propagation through the PSP to the west of Taiwan gives seismic intensity at strong motion stations only on the east coast with a PGA range of 3.6–19.4 cm/s². PGA values can be obtained from broadband stations BATS and CWBSN networks in other area, with a maximum value of 2.8 cm/s² (Figure 2c). The high-frequency P and S wave signals are also observed in the coastal stations, e.g., ECL (fore-arc side) with a striking contrast to back-arc side station such as ANP (Figure 2f). Evidence of wave guiding in northern Taiwan and southern Japan occurs in the same subducted PSP for a single event, which exhibits similar high-frequency guiding properties examined by taking a spectral ratio of guiding and non-guiding seismograms (Figures 2e and 2g) with linearly increasing spectral ratio from 1 to 10 Hz.

[8] The observed high-frequency signals and anomalous PGA pattern during this intermediate-depth earthquake in Figure 2 confirm the guiding of waves in the PSP, parallel to the trench, for long travel distances in both directions. Such guiding effects from deeper events in the PSP and Pacific plate are well recognized in Japan and can be explained by multiple scattering of seismic waves due to anisotropic heterogeneity of elongated properties in the slab [*Furumura and Kennett*, 2005; *Furumura and Kennett*, 2008]. However, in the western PSP, the propagation characteristics of the PSP waveguide to Taiwan and the association with ground shaking intensity levels have not been characterized. Note that in northeastern Taiwan, subduction is superimposed with collision where the westernmost edge of the Ryukyu trench terminates against Taiwan to meet the Eurasian lithosphere near 122°E, 24°N in Figures 1a and 1b. In this case, the seismic stations lie to either west of the PSP edge or above EP lithosphere, so that guided energy may be coupled into the crustal waveguide rather easily. Seismograms from even a deeper subduction event can appear similar to a crustal event at a larger epicentral distance, as a result of crustal scattering merging into guided waves propagating in the slab. Compared with the well-demonstrated characteristics of guided waves within the Pacific plate of the Japan subduction zones for events below 200 km depth [*Furumura and Kennett*, 2005], the length of guiding in the subducted PSP is quite short. This is because most PSP earthquakes near Taiwan occurred above a depth of 200 km, which leads to a limited possibility of enhancement of high-frequency energy. These facts complicate the observation and analysis of guiding waves in Taiwan and therefore make the characterization of guided waves in this area challenging.

3. Anomalous Distribution of Seismic Intensity From Intermediate-Depth Events

[9] To better understand the nature of the guiding effect of the PSP near Taiwan, an examination of a larger number of guided wave events is necessary. Figure 1 shows the distribution of $M > 5$ earthquakes during the period of 1996 to 2009. In this map, the subducting PSP is illustrated by iso-depth contours, and the distribution of BATS broadband stations across Taiwan are shown by black triangles. Good coverage of seismic stations and frequent earthquake activity provide an opportunity to explore wave propagation and attenuation behavior associated with strong heterogeneities in the crust and upper mantle structure of subduction zones underneath Taiwan. In this study, 98 $M > 5$ earthquakes in the latitude range 24.2°–25.5°N and longitude range 121.5°–124.0°E are analyzed, hereafter referred to as "PSP events." Their epicentral region is enclosed by the dashed box in Figure 1, where the $M > 5$ events with good signal to noise level with waveforms recorded at more than five stations are shown by filled circles.

[10] Figure 3 illustrates the comparison of PGA patterns for shallow and intermediate-depth earthquakes with different focal mechanisms. Unlike shallow earthquakes that exhibit normal seismic intensity distribution with strong shaking concentrating near the epicenter and intensity decaying gradually with epicentral distance (Figures 3a–3c), intermediate-depth earthquake from subducted PSP adjacent to Taiwan reveals abnormally strong intensity (Figures 3d–3f) displaced from the closest point on land. In Figure 3d, the PGA map for the 175 km deep event shows a distorted pattern extending southward to stations TDC and CHG. Such an abnormal PGA pattern can be found in all intermediate-depth events occurring in the PSP for a variety of focal mechanisms. The PGA contours from the three intermediate-depth events with normal, strike-slip, and thrust faulting mechanism exhibit a common southwest elongation with large PGA value at TDC station which is several times greater than that at ANP station both about ~100 km from the epicenter. The consistently anomalous extension of PGA pattern in Figures 3d–3f suggests that such anomaly does not require a specific radiation pattern for the S wave. Also, the anomalous PGA zone is larger than 100 km, which is unlikely to be a result of a localized site amplification effect. The abnormal distribution of seismic intensity from intermediate-depth PSP events therefore indicates that there needs to be large-scale anomalous attenuation structure in the crust and mantle, rather than in the shallow structure which would produce localized site amplification effects.

4. Nature of Waveforms and Frequency Content for Events With Apparent Guiding

[11] To understand the cause of the distorted PGA patterns, we examine the waveform characteristics of the intermediate-depth events in the PSP. The seismograms recorded in the area of large seismic intensity are found to show relatively high-frequency energy in both P and S wave trains as compared with the seismograms recorded at similar epicentral distances but outside the area of large intensity. As shown in Figure 4, the intermediate-depth $M7.1$ event reveals larger PGA values (i.e., >50 gal) across stations YHN, NNS, TDC, NAC, CHG, and HWA, where the seismograms are visually characterized by higher-frequency content compared with stations located outside the area with larger PGA (Figures 4b and 4c). Thus, there is a connection between anomalous ground motion and frequency content of the seismograms. Even though it might be expected that such anomalous PGA value could be caused by site amplification effect, note that the BATS broadband stations are mostly placed in hard rock, whereas the stations showing strong guiding phenomena are placed on igneous and metamorphic rocks, limestone, and hard volcanic deposits (see site geology condition at http://bats.earth.sinica.edu.tw/Station/BATS_Stn_Summary.html). Superposition of BATS stations and the strong motion site amplification map of *Lee et al.* [2001] also illustrates that the guiding phenomena appear in strong motion stations at type B site class (rock, $Vs = 760$–1500 m/s) so that the site amplification
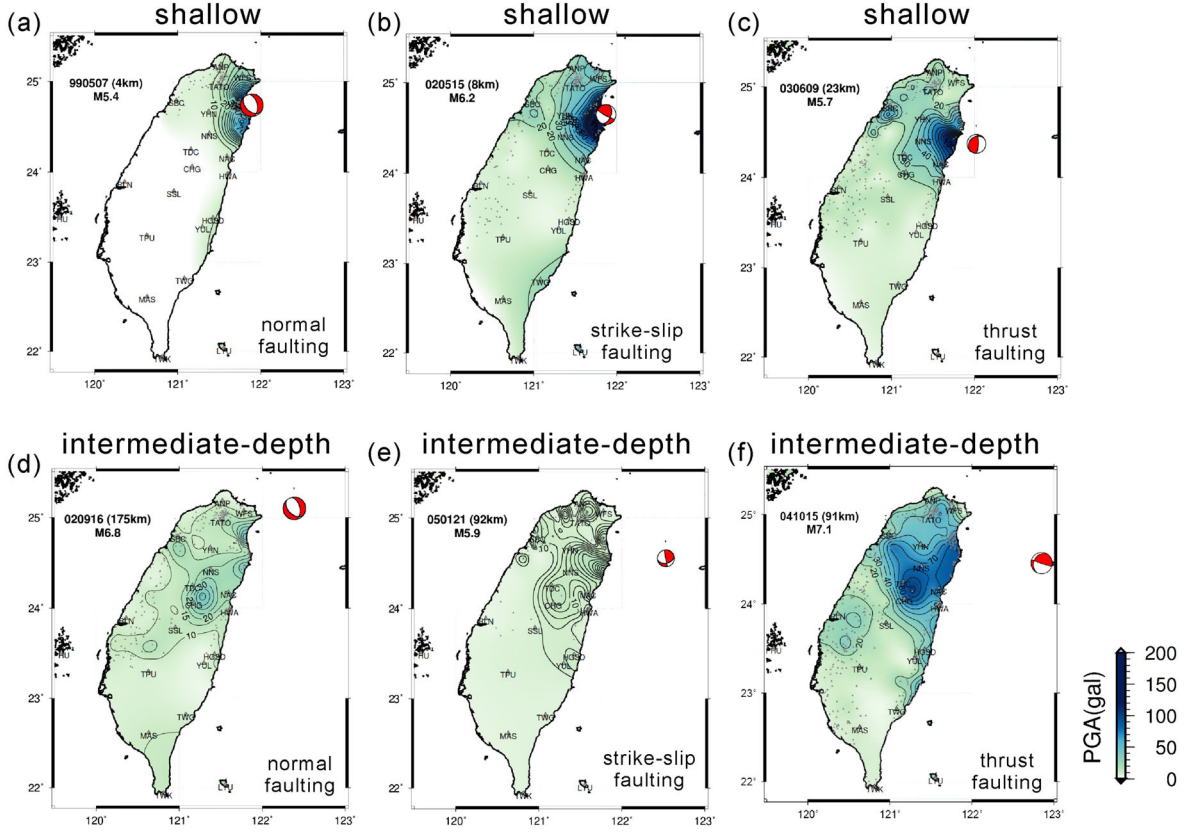
Figure 3. Horizontal PGA distribution map for shallow (a–c) and intermediate-depth(d–f) earthquakes with a variety of focal mechanisms. (a, d) Normal faulting events with different focal depth, 4 km and 175 km. (b, e) Strike-slip faulting events with focal depth of 8 km and 92 km. (c, f) Thrust faulting events with focal depth of 23 km and 91 km. Darker tones indicate more intense acceleration.
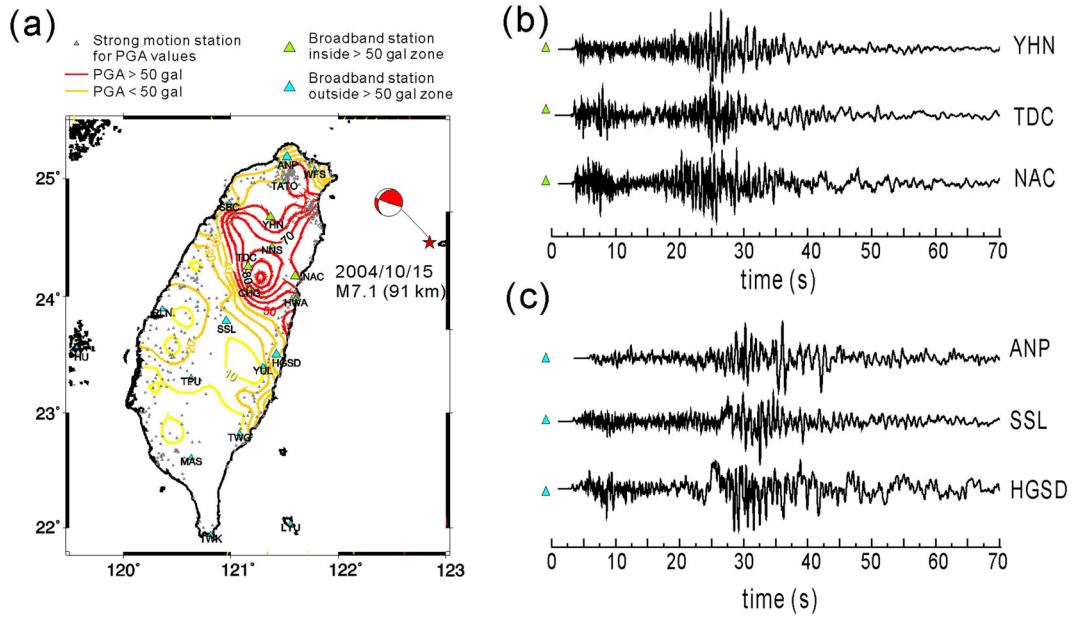

Figure 4. (a) Hypocenter of an intermediate-depth event (Figure 3f) offshore northern Taiwan and the anomalous PGA pattern represented by contours. Small gray triangle indicates the strong motion stations used to compute horizontal PGA values. Green and blue triangles indicate broadband stations for seismograms. (b and c) Vertical component seismograms for stations inside and outside the PGA > 50 gal zone are shown in Figures 4b and 4c, respectively.

factor is not so significant (see Figure S1 in the Supporting Information).

[12] In Figure 5, we schematically illustrate the configuration of the propagation paths for shallow and intermediate events at the same stations. At station TDC near the western edge of the subducted PSP, there is strong high-frequency energy with long coda for the intermediate-depth event but not for the shallow event. On the other hand, such elevated high-frequency energy observed at TDC station for the intermediate-depth event does not appear at ANP station located to the other side of subducted slab (Figure 5a). This indicates substantial differences in attenuation structure along these wave propagation paths in the northern Taiwan subduction zone, which is characterized by large contrast between high-V, high-Q slab and low-V, low-Q surrounding mantle.

[13] Figure 6 shows the spectra and spectral ratio for a 10 s P wave window at the stations TDC and ANP for shallow and intermediate-depth events. The spectra at TDC station reveals amplified energy at the frequency of 3 Hz with a significant increase of amplitude at higher frequency. For the intermediate-depth event, the TDC/ANP ratio reaches a maximum at ~10 Hz with a ratio of 300 (Figure 6a). In contrast, the shallow earthquakes do not show such a dramatic increase of amplitude at higher frequency (>3 Hz), and both TDC and ANP reveal similar amplitudes with a decaying spectrum at higher frequency (Figure 6b). In the $M > 5$ earthquakes examined, the energy higher than 3 Hz is amplified by a factor of 4–400 compared with the back-arc station ANP. Elevated high-frequency energy is also found at some other stations (e.g., SSL and NAC), which confirms the association with the high-frequency wave guide effect of the subducting slab, instead of localized site amplification.

Such a slab-guiding effect is expected to be more evident for S wave characterized by shorter wavelength and lower wave speed compared with P wave. This is enhanced by the greater efficiency in P to S scattering process so that the apparent character of the coda is likely to become richer in S wave.

[14] Figure 7 displays vertical, radial, and transverse components of broadband seismograms from a PSP event at stations NAC and TDC where the large ground motion acceleration is observed for intermediate-depth events in Figure 3. High-frequency signals with sustained P and S wave coda appear on all three components, suggesting that the small-scale heterogeneity in the plate with wavelength comparable to the high-frequency signals may facilitate strong internal scattering to develop long high-frequency coda. There also appears to be a low-frequency forerunner to the P wave arrival (around 0.5 Hz) and followed by higher-frequency coda (>3 Hz). The low-frequency P wave onset is only recognized in the radial and vertical components but not in tangential motion. As also indicated by polarization analysis of a low-frequency onset recorded at stations NAC and TDC particle motion in Figures 7c and 7e, there appears to be significant amount of energy on vertical and radial components. This indicates that the first arrival of low-frequency signal is from the direct propagation of the source to the station along the great circle path.

[15] The later high-frequency P wave coda (>3 Hz) appears on all three components with comparable amplitude, indicating that strong scattering of high-frequency signals occurs with a waveguide effect. Based on finite-difference method simulations of high-frequency seismic wave propagation to frequencies up to 18 Hz by *Furumura and Kennett* [2005], anisotropic, small-scale heterogeneity with elongated structure in the slab
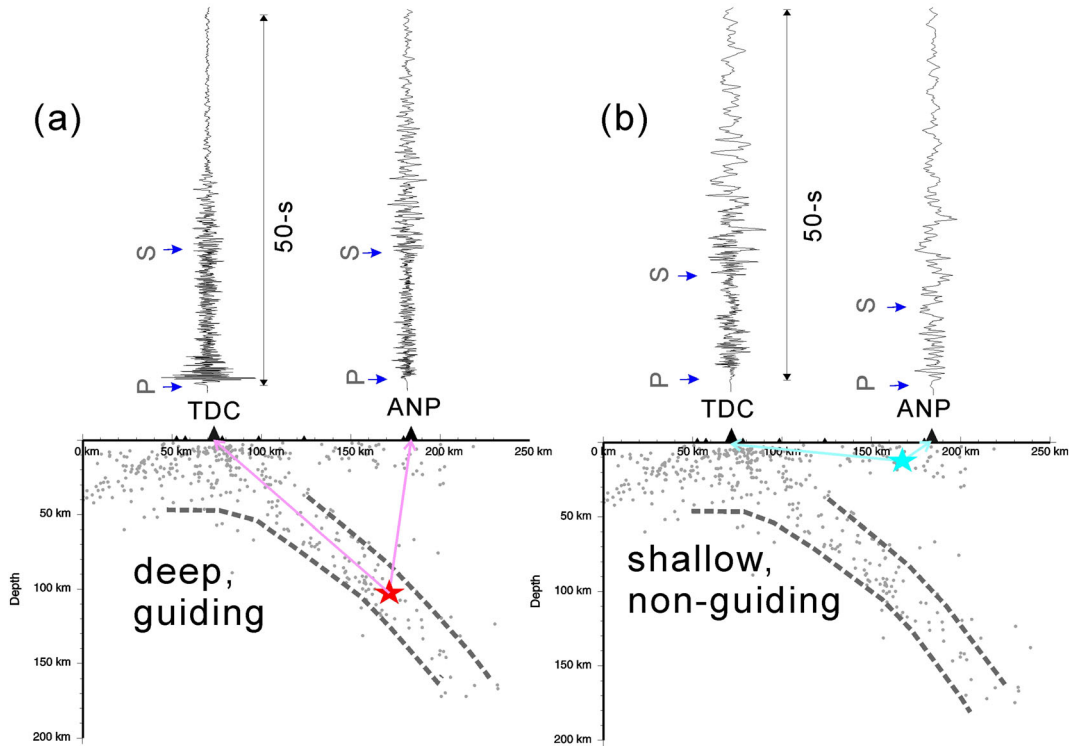

Figure 5. Schematic representation of propagation paths for events with the presence and absence of guiding and comparison of waveforms. (a) The intermediate-depth earthquake at a depth of 120 km (17 May 2005 M5.1). (b) The shallow earthquake at a depth of 7 km (13 June 2002 M5.0).
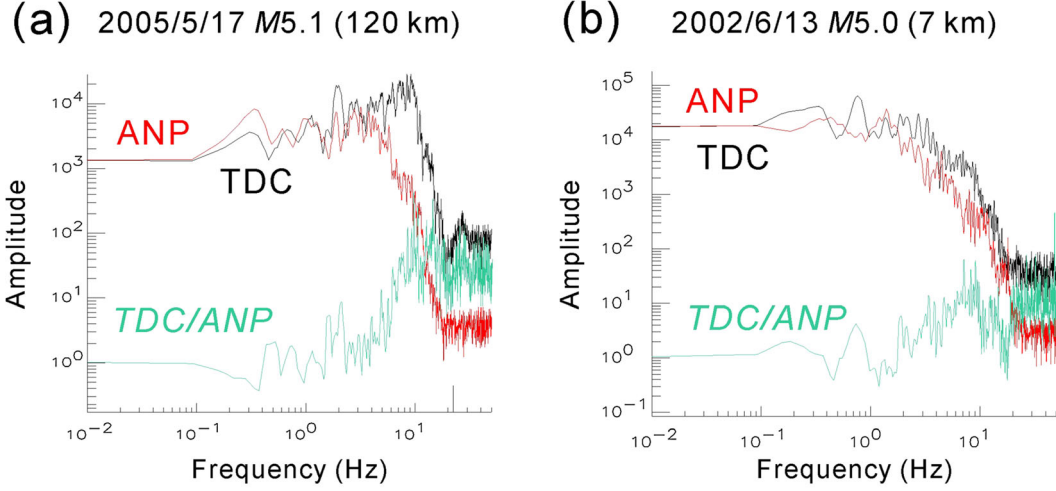
Figure 6. Fourier spectrum of the broadband waveforms at TDC station with guided waves and ANP station where no subduction guiding is evident for (a) intermediate-depth earthquake and (b) shallow event as indicated in Figure 5. The spectral ratio of TDC relative to ANP is shown by a green line.

plays an important role for the scattering and guiding of high-frequency seismic waves during the propagation to greater distances. They also demonstrated that the peculiar observation of a low-frequency onset followed by high-frequency long coda is developed during the guiding along the slab due to multiple diffraction of seismic wave in the slab with anisotropic heterogeneity.

5. Depth-Dependent Guiding Behavior

[16] At station TDC where the pronounced PSP guided effect is observed, the frequency content changes with the depth of the event. This can be seen in a display of seismograms with varying focal depth in Figure 8a. Long-lasting, high-frequency signals appear for event depths greater than 60 km. The contrast in dominant frequency for shallow (<60 km) and deeper (>60 km) events is striking. Note that the magnitude of these events is confined in the range from $M5.0-6.0$ except for the 6 August 2007 $M6.6$ event at 54 km depth. As shown in Figure 8b, the seismic waves for events deeper than 60 km are made up predominantly of high frequencies in the range of 4-10 Hz, whereas the shallower events have limited >3 Hz energy. The presence of amplified high-frequency signals for intermediate-depth events suggests the enhancement of high-frequency energy (at a range of 3 to 10 Hz) while traveling along the subducting PSP. The spatial distribution of BATS stations showing a guiding effect (i.e., depth-dependent frequency content as illustrated in Figure 8b for spectra and Figure S2 for spectrograms) is shown in Figure 7a (orange and red triangles). Clear slab-guiding influences are observed at stations WFS, YHN, NAC, TDC, SSL, and YUL, where the high-frequency energy (3–10 Hz) appears for deeper than 60 km earthquakes but not for shallow events.

[17] The guided wave events with apparent low-frequency first arrivals are selected and displayed in Figure 9. We find a clear separation between low-frequency onset (<1 Hz) and high-frequency (>3 Hz) onsets (called "dt" hereafter) that behave differently at different stations. Here the interval dt is measured by the time separation of the first motions

between low-frequency arrival and high-frequency second arrival (see Figure 9 for example). In stations TDC and NAC, the dt ranges from 0.0 to ~0.5 s, whereas at station SSL, the dt is relative large up to 0.72 s. As illustrated by Figure 10, the dt for stations SSL and TDC seems to slightly increases with focal depth and travel distance, whereas NAC station does not reveal any systematic trend.

[18] If the dt is measured by the arrival of the main wave train (larger amplitude arrival) rather than the first motion, the dt ranges for TDC and SSL stations are 0.3–0.6 s and 1.0–1.3 s, respectively (Figure 9). Note that the travel distance to SSL station is longer with additional travel path in the continental crust compared with TDC stations. So the greater high-frequency energy arriving much later at SSL and TDC station can be a result of the summation of multiple scattering and diffraction for longer propagation in the heterogeneous slab.

6. Quantification of Subduction Zone Guided Waves

[19] While traveling up the subducted slab, the high-frequency coda of P and S phases is built up by patterns of multiple reflections and scattering, which is described as a plate guiding effect. As illustrated in previous sections, the guiding effect is represented by dominance of high-frequency energy and the long duration of coda. Recognition of guided wave phenomena in previous sections provides useful information for an empirical quantification method.

[20] We conduct moving-window spectral analysis to obtain the ratio of high- to low-frequency signals. This is done by computing spectrum for each seismogram using windows 5 s long, stepping forward at 4 s increments through 61 s after the P arrival. The median amplitude of spectra for high-pass filter with 5 Hz and low-pass filter with 4 Hz is used to determine an *hp/lp ratio* by the following equation:

$$hp/lp\ ratio = A_{>5\ Hz}/A_{<4\ Hz}, \tag{1}$$

where A represents the median value of the Fourier spectra amplitude. The *hp/lp ratio* for every spectrum is plotted as a function of time along the seismogram. Figures 11a–11c show
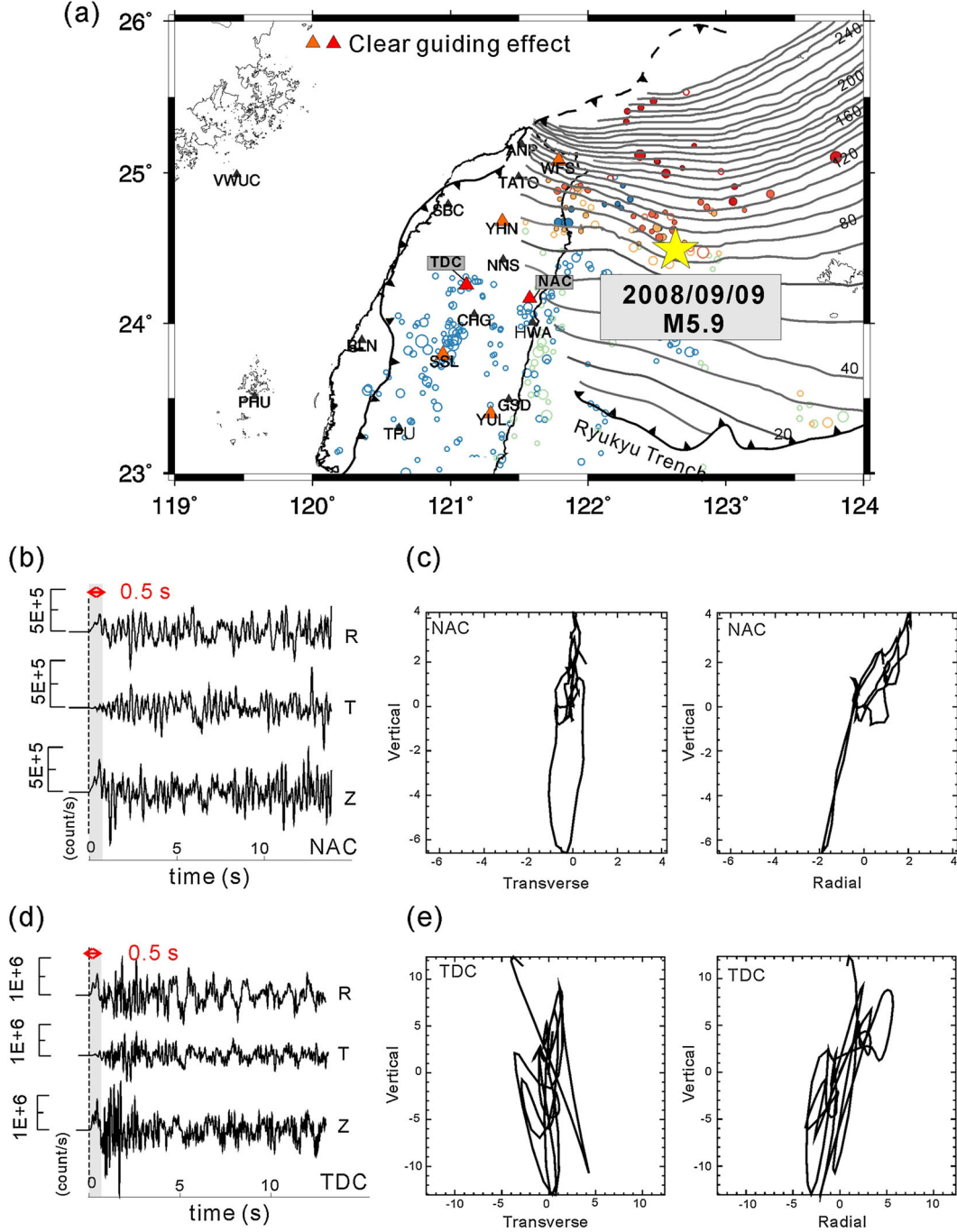
Figure 7. (a) Distribution of stations showing clear guiding effect (orange and red triangles) from subduction zone events with depth-dependent high-frequency content (example shown in Figure 8). Also shown is the epicenter for an intermediate-depth PSP event (9 August 2008 M5.9, 104 km depth). The stations NAC and TDC are highlighted in red. (b) Vertical (Z), radial (R), and transverse (T) components of seismograms for 15 s long seismogram starting from P wave arrival at station NAC. (c) Particle motions of the vertical, radial, and transverse components in Figure 7b, using 0.5 s window from P arrival. (d) 15 s long seismograms starting from P wave arrival at station TDC. (e) Particle motions of the vertical, radial, and transverse components in Figure 7d, using 0.5 s window from P arrival.

examples of the *hp/lp ratio* for three different seismic networks: broadband TAIGER (Taiwan Integrated Geodynamics Research), short-period CWBSN, and broadband BATS (station distribution shown in Figure 11d). The stations characterized by a clear guiding effect (i.e., depth dependency of sustained high-frequency signals) are shown by colored curves, whereas stations showing no clear guiding effect are shown by gray. The *hp/lp ratio* is expected to decay with time as the high-frequency component diminishing more efficiently compared with low-frequency energy. On the other hand, anomalous
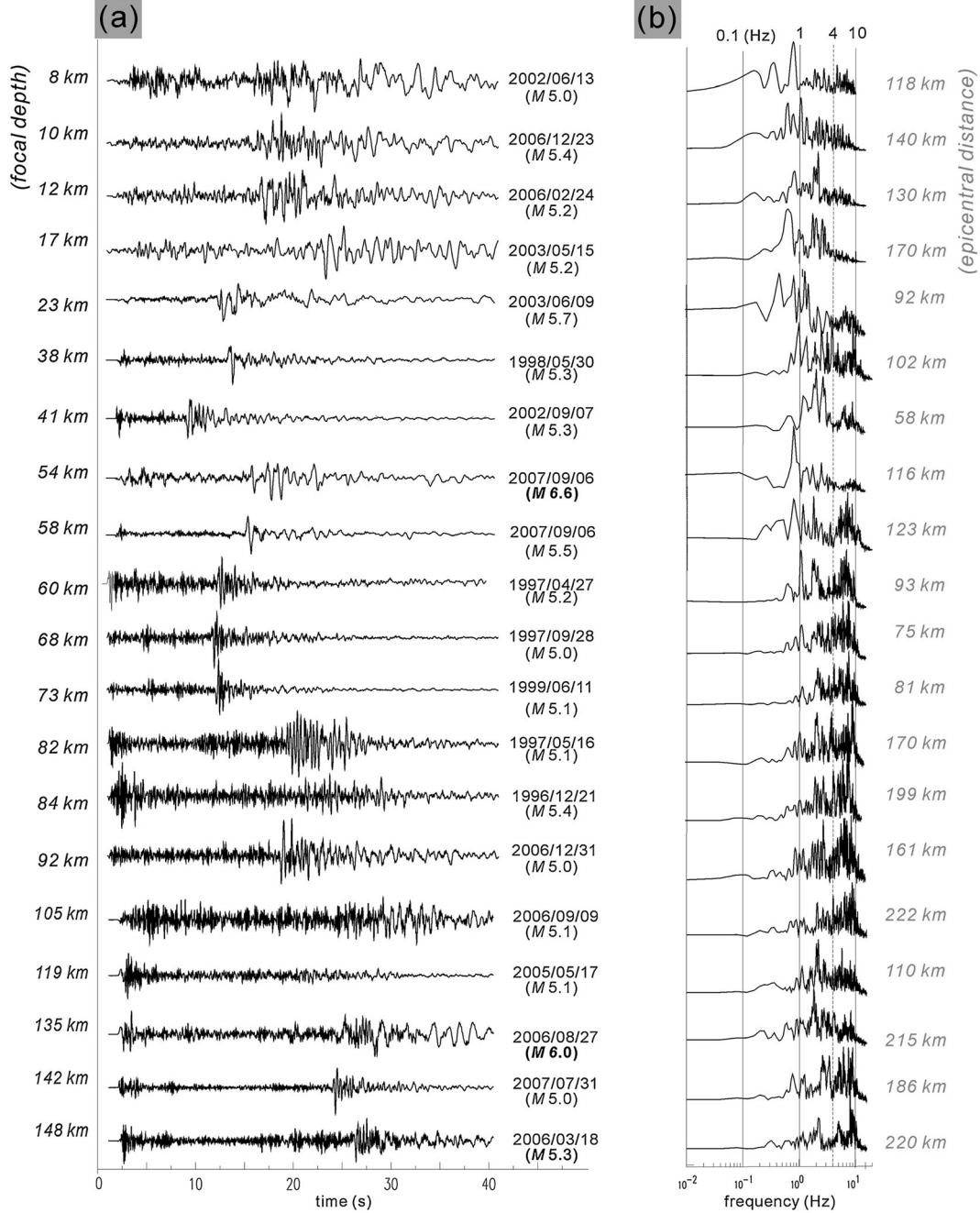
Figure 8. (a) shows 40 s window of unfiltered vertical-component broadband seismograms recorded at TDC station with aligned *P* onsets from events at a variety of depths. Occurrence time and magnitude for each event are also shown. (b) The corresponding spectra using 10 s window starting from 0.5 s before *P* arrival. Number on the right indicates the epicentral distance.

phases with long high-frequency coda (guiding effect) can be presented by a higher *hp/lp ratio* over a longer time span.

[21] In Figures 11a–11c, the stations with a guiding effect appear to have *hp/lp ratio* greater than 2 (denoted by horizontal dashed line) starting immediately from *P* arrival. The duration for which the *hp/lp ratio* > 2 differs between stations. Figure 11d shows the spatial distribution of stations with *hp/lp ratio* > 2, color coded by their duration. The stations defined by a *hp/lp ratio* > 2 are concentrated along the east coast, with longer than 15 s duration located near the Ryukyu trench. The most efficient slab guiding is found at the

TGC11 and TDC10 stations characterized by the longest duration of higher-frequency signals, at latitude 23.7°, and the guiding effect diminishes rapidly in southern stations. This may provide a hint as to where the Ryukyu subduction boundary intersects with Taiwan, indicated by the dashed line connected to the western end of the bathymetrically well-defined Ryukyu trench in Figure 11d. The spatial pattern of the *hp/lp ratio* is also found to be consistent with the common PGA pattern for intermediate-depth events shown in Figures 3d–3f. This suggests that the anomalous peak ground motion from intermediate-depth events in
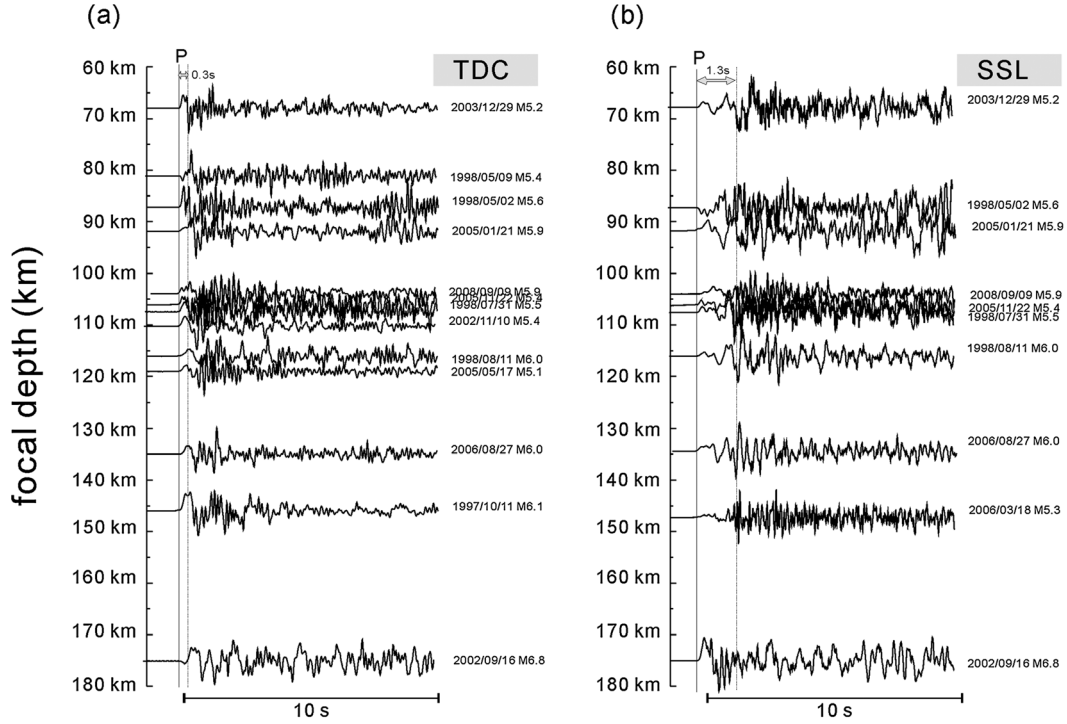
Figure 9. Seismograms with aligned *P* onsets of low-frequency forerunner for events with varying focal depth (10 s window of unfiltered vertical-component broadband seismograms) at TDC and SSL stations. The first vertical line denotes the aligned low-frequency first arrival. The second vertical line indicates the higher-frequency onset picked for the 68 km depth event.
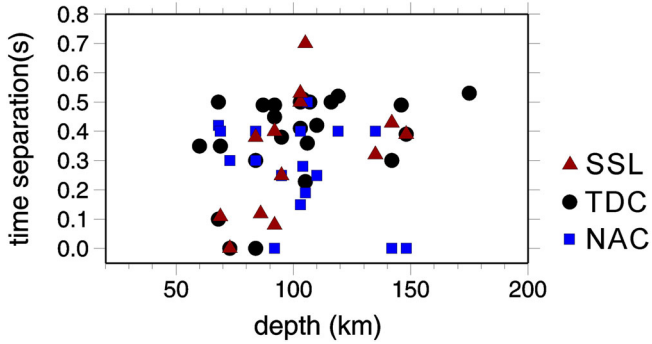

Figure 10. Time separation between the low- and high-frequency arrivals as a function of focal depth for SSL, TDC, and NAC stations.

the area offshore northeast Taiwan is coupled with a PSP guiding effect.

7. Discussion

7.1. Indication of Subducted EP Guiding Effect

[22] The northern extension of the eastward dipping Eurasian slab underneath Central Taiwan has been controversial. If the collision between the Chinese Continental Margin and the Luzon Volcanic Arc involves the entire EP lithosphere, then one should expect an absence of slab in Central Taiwan [*Wu et al.*, 1997]. If the orogeny is a result of accretionary wedge deformation over a passively subducting lithosphere, then the presence of slab of is expected [*Suppe et al.*, 1981]. A tear fault that cut through the continent-ocean boundary

is also proposed, to explain how the two subducted plates meet underneath Central Taiwan [*Lallemand et al.*, 1997; *Lallemand et al.*, 2001]. There are mounting evidences from tomography [*Wang et al.*, 2006, 2009], secondary *P* phase [*Lin*, 2009], seismic velocity anomaly, and receiver-side waveform effect from teleseismic *P* waveforms [*Chen et al.*, 2004; *Chen et al.*, 2011; *Chen et al.*, 2012] that suggest the subducted EP can be followed up to latitude 24°N, through there are differences in slab configuration.

[23] Guided waves may provide independent information for the geometric configuration of the subducted EP underneath Central Taiwan. The spatial distribution of the guiding stations can be an indicator for possible plate geometry of EP beneath southeastern Taiwan. However, unlike the common near-land seismicity in PSP, the EP events occur further offshore and only limited number of events has been recorded well at inland stations. Our examination of a number of EP events reveals clear guiding behavior. As shown in Figure 12, an EP event at 170 km depth shows sustained high-frequency signals on all three components, with a clear low-frequency first arrival seen on radial and vertical components but the diminished energy of low-frequency onset on transverse component (Figure 12b). The big contrast in frequency content between shallow and deeper events can be clearly seen at stations TPU and TWG (Figures 12c–12d), where only EP events deeper than 90 km reveal long high-frequency coda. The PGA distribution for EP events also reveals depth-dependent behavior. As illustrated in Figure 13, the intermediate-depth EP event shows westward elongation of the strong PGA, whereas the shallow event has strong PGA concentrating near the epicenter. There is an open question whether such
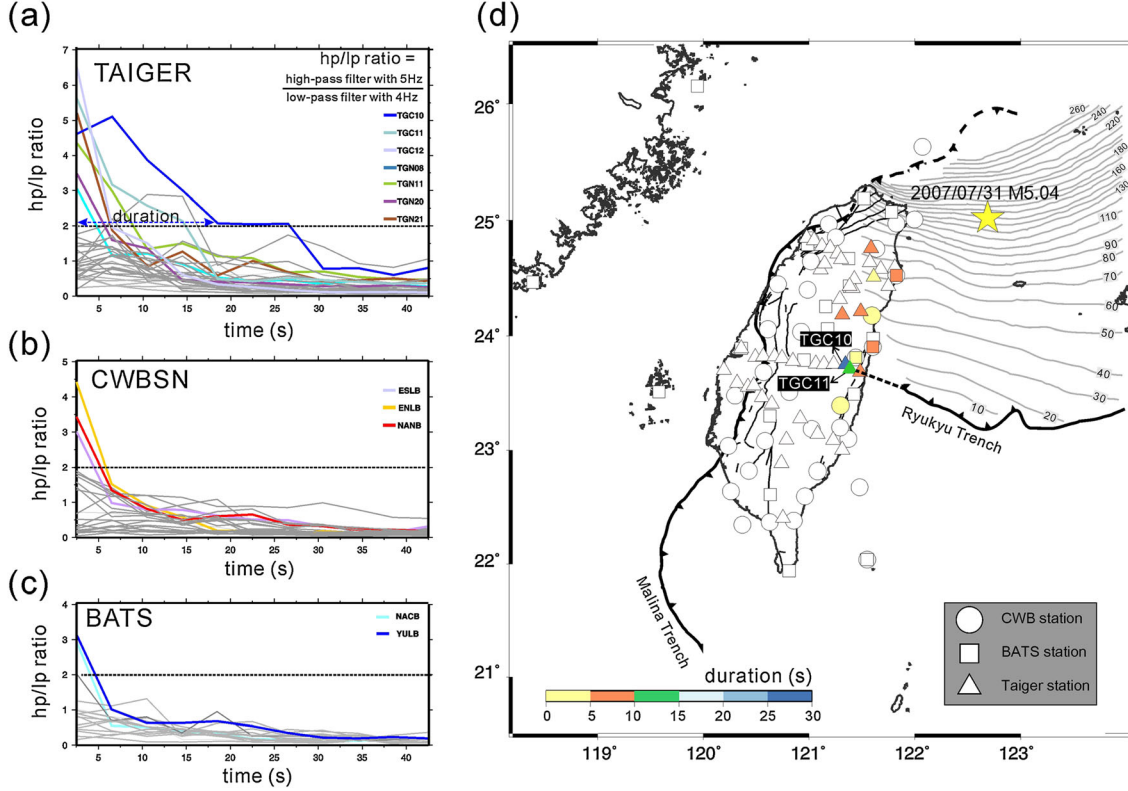
Figure 11. *Hp/lp* ratio as a function of time for seismograms from different networks: (a) TAIGER, (b) CWBSN, and (c) BATS. Colored lines denote stations showing apparent guiding, whereas gray lines indicate no apparent guiding. (c) Spatial distribution of significant guiding effect. The guiding effect is defined by the ratio of high-pass filter with 5 Hz to low-pass filter with 4 Hz. Earthquake is chosen for M5.0 event occurred on 31 July 2007 (depth: 142 km).

an elongation of the intensity contours is associated with a fold of the Eurasian plate crust underneath eastern Taiwan. If so, we would expect the guided waves to be observed at stations along the east coast or on the eastern flank of Central Range. The observed seismic waveform characteristics, however, reveal partial guiding across the southern portion of Taiwan and along the east coast, suggesting some of the high-frequency energy may couple into the crust.

[24] To confirm that the high-frequency coda is due to guided waves in the subducting slab rather than localized site amplification effects, more complete data collection for exploring depth-dependent EP guiding behavior is necessary. Further studies of the similarities/differences in the plate waveguide for PSP and EP will provide useful information towards the fundamental understanding of slab properties continuity underneath Taiwan.

7.2. Worldwide Slab-Guided Wave Phenomena

[25] The cooler slab of the subducted lithosphere is a high-velocity body compared with the ambient mantle, which allows the seismic waves traveling through to arrive early at the surface. In addition, the low-attenuation (high-Q) slab allows the seismic wave to travel longer distances with lesser attenuation than that propagating outside the slab. The low-velocity structure at the top of the slab complicates the wavefield to trap high-frequency signals within and facilitates dispersion of medium-frequency signals due to the large velocity contrast with the surrounding high-velocity

zone. Such heterogeneous structure of the subducting slab often generate large, long-lasting high-frequency signals that cause anomalous seismic intensity patterns with a significant extension of intensity contours along the plate [e.g., *Utsu*, 1966; *Furumura and Kennett*, 2005].

[26] Such slab-guided waves have been recognized in worldwide subduction zones with different classes of guided wave phenomenon and different models to explain the guided wave effects: (A) a slab-guided wave with small-amplitude low-frequency precursor following large-amplitude high-frequency signals which is developed by low-velocity former oceanic layer on the top of the subducted plate, named *LVL* [*Fukao et al.*, 1983; *Hori et al.*, 1985; *Oda et al.*, 1990; *Abers*, 2000; *Martin et al.*, 2003; *Martin and Rietbrock*, 2006]; (B) a slab-guided wave with small-amplitude high-frequency forerunner following large-amplitude high-frequency signals developed by high-velocity layer in the interior of the subducted plate [*Barazangi et al.*, 1972; *Ansell and Gubbins*, 1986; *Gubbins and Snieder*, 1991; *Gubbins et al.*, 1994; *van der Hilst and Snieder*, 1996], named *HVL*; and (C) slab-guided wave with a low-frequency precursor and following large-amplitude high-frequency long-duration signals developed by multiple forward scattering of high-frequency signal in elongated small-scale heterogeneities inside the plate [*Furumura and Kennett*, 2005, 2008], named ES. The characteristics of these three types of slab-guided waves in observations from around the globe are listed in Table 1 and discussed below.
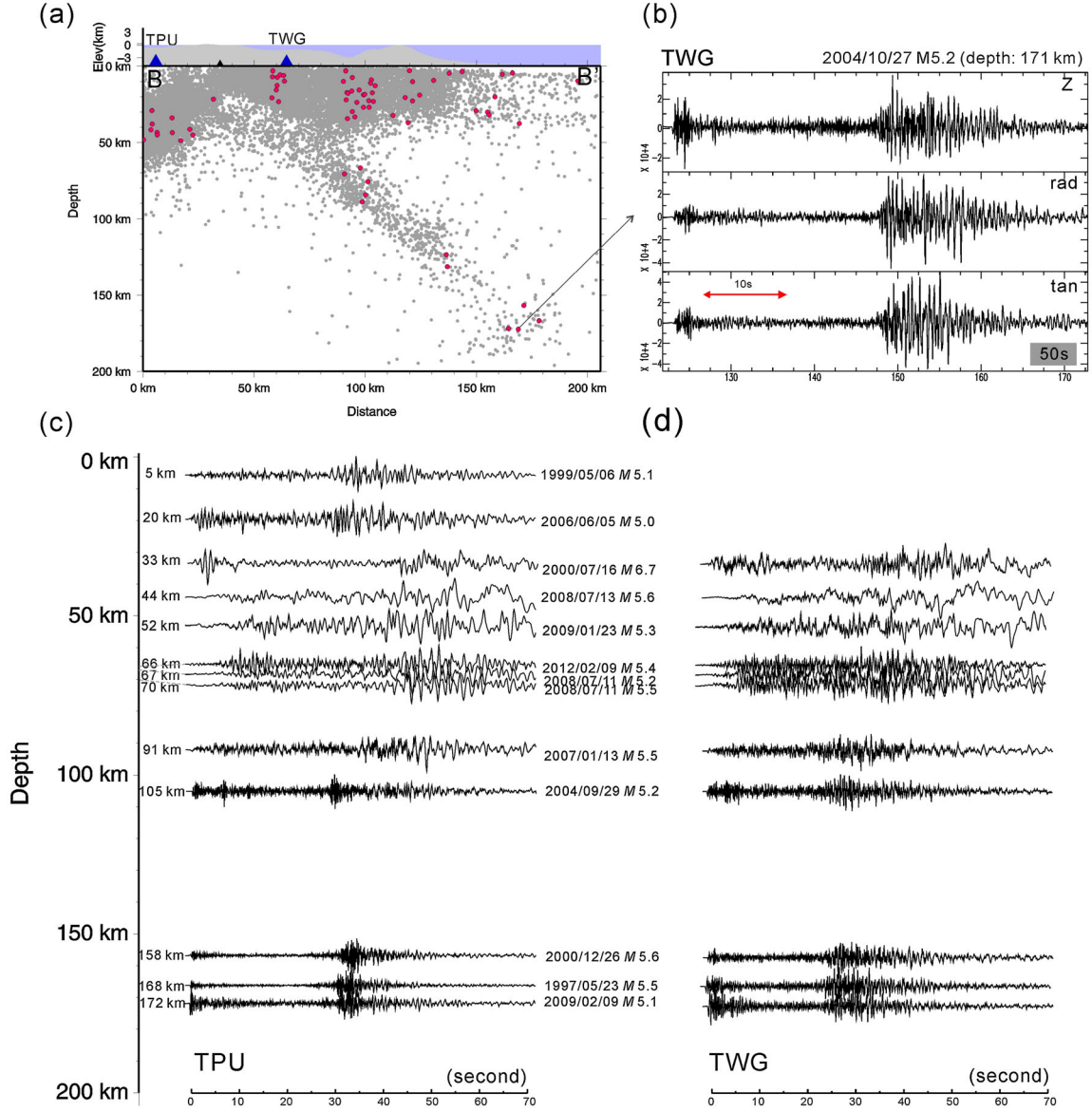
Figure 12. (a) Cross sections showing background seismicity (1991–2009) along profiles B-B′ in Figure 1. Red and circles indicate the $M \geqq 5$ and $M \geqq 2$ events, respectively. (b) Vertical, radial, and transverse components of seismograms for a EP event (M5.2 event occurred on 27 October 2004 with focal depth of 170 km) with guiding behavior recorded at TWG station. (c and d) show 70 s window of unfiltered vertical-component broadband seismograms recorded at TPU and TWG stations at a variety of depths.

[27] The type A guided wave due to LVL is widely observed associated with a low-frequency precursor (i.e., low-frequency phases arriving earlier than the higher-frequency later phases) in many subduction zones (Table 1). Along the Nankai-Trough of western Japan where PSP subducts show first arrival of small-amplitude low-frequency signals following large-amplitude high-frequency *P* and *S* wave signals [*Fukao et al.*, 1983; *Hori et al.*, 1985; *Oda et al.*, 1990] from intermediate-depth earthquakes no deeper than 60 km. The cause of the guiding was first explained by *Fukao et al.* [1983] as the fast arrival is a refracted wave along the interface of low-velocity former oceanic layer and high-velocity oceanic mantle, while later large-amplitude signal is the trapped signals propagating in the oceanic layer. Such waveguide effect disappears for deeper earthquakes since

the low-velocity former oceanic layer cannot survive beyond a depth of about 100 km, because the dehydrated material at that depth is expected to transform to high-velocity ecologite for the PSP of the Nankai-Trough at that depth [*Fukao et al.*, 1983]. In the North Pacific subduction zones, similar waveguide property for in-slab earthquakes are observed with a time delay between the high-frequency (>3Hz) and low-frequency (1–3 Hz) arrivals in a range of 1.5–2 s for much deeper events between 100 and 250 km, where a low-velocity former oceanic layer with thickness of 1–7 km at the top of the high-velocity slab is inferred to explain the time separation [*Abers*, 2000]. In the Chile-Peru subduction zone, the time delay between >5 Hz and <2 Hz signals is about 1 s for 110–140 km events [*Martin et al.*, 2003; *Martin and Rietbrock*, 2006], where a source located in the former oceanic layer is
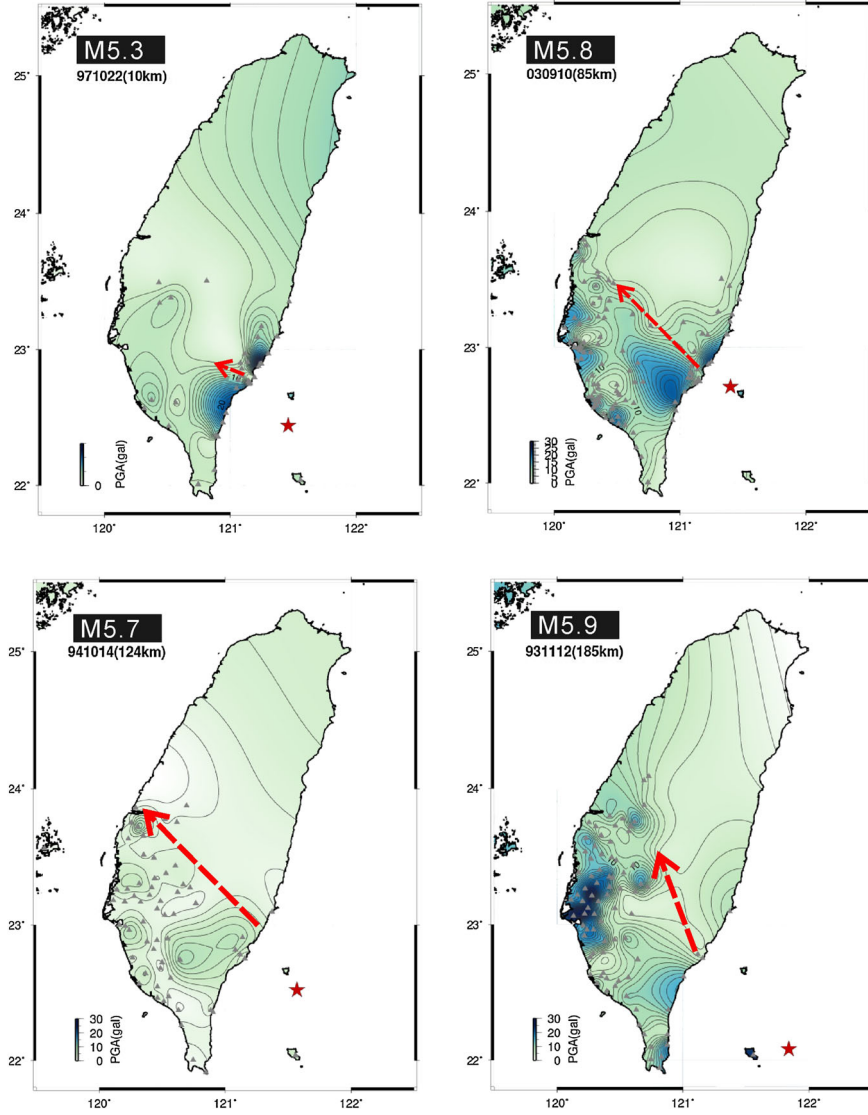
Figure 13. Horizontal PGA distribution map for EP events with a variety of focal depths. (a) 22 October 1997 M5.3 earthquake at a depth of 10 km. (b) 10 August 2003 M5.8 earthquake at a depth of 85 km. (c) 14 October 1994 M5.7 earthquake at a depth of 124 km. (d) 12 November 1993 M5.9 earthquake at a depth of 185 km. Red star indicates the epicenter of the main shock. Red dashed line denotes the direction of PGA extension. Gray triangles indicate the strong motion stations used for PGA values calculation.

required in their models to match the early arriving low-frequency wave train. Dispersion of medium-frequency seismic waves with faster propagation of lower-frequency signals than high-frequency signals is also seen in the Hellenic subduction zone [*Essen et al.*, 2009], where the trapped structure of low-velocity oceanic crust is believed to be a cause of guiding of the high-frequency signals. Based on simulation by *Martin et al.* [2003], the guided wave can be easily developed for (1) the longer travel distance within the low-velocity layer, (2) source located within or closer to the low-velocity layer, (3) thin enough waveguide, and (4) a large velocity contrast of the low-velocity layer with the ambient mantle.

[28] The type B guided wave is found to be associated with a high-frequency precursor (i.e., small-amplitude, high-frequency first arrivals with several seconds separation from the following low-frequency, large-amplitude arrivals) for intermediate and deep earthquakes propagating along the slab [*Chiu et al.*, 1985; *Shin*, 1992, *Ansell and Gubbins*, 1986; *Gubbins and Snieder*, 1991; *Galea*, 1992; *Smith et al.*, 1994; *Stuart et al.*, 1995; *van der Hilst and Snieder*, 1996]. It has been inferred to be a result of thin high-velocity layer only a few km (named HVL). The amplitude and frequency content strongly depends on the thickness of the HVL [e.g., *Smith et al.*, 1994; *van der Hilst and Snieder*, 1996; *Chang and Huang*, 2002], though it is rather difficult to keep high-frequency waves over long distances in HVL. *Sugioka et al.* [1996] found the presence of high-frequency precursors from earthquakes in Kamchaka and Ryukyu island. Based on the 2-D simulation by *van der Hilst and Snieder* [1996] and 3-D wave propagation model by *Chang and Huang* [2002]; the generation of such high-frequency precursors requires (1) source located within a thin and continuous HVL, whereas the thinner HVL leads to smaller amplitude and higher frequency of the precursor; (2) a specific

Table 1. Worldwide Slab-Guided Wave Phenomena

Slab-Guided Wave Type	Observed Characteristics First Arrival/Later Arrival/Time Separation	Subduction Zones	Depth Range Showing Guiding Phenomenon	References
A	Distinct later phases at coastal stations but not inland stations	Western Japan	<100 km	*Fukao et al.* [1983], *Hori et al.* [1985], and *Oda et al.* [1990]
A	1–3 Hz/>3 Hz/1.5–2 s	North Pacific subduction zones (Kuril, Alaska, Aleutian, northern Japan, Mariana)	100–250 km	*Abers and Sarker* [1996] and *Abers* [2000]
A	<2 Hz/>5 Hz/~1 s	Chile-Peru	110–140 km	*Martin et al.* [2003]
A	~0.5 Hz/~3 Hz (single event)	Hellenic	—	*Konstantinou and Melis* [2008] and *Essen et al.* [2009]
B	High-f/low-f character (*P* to *S* conversion)/2–3 s	Vanuatu	70–260 km	*Chiu et al.* [1985]
B	Small amplitude >2 Hz/<1 Hz/>2 s	New Zealand (Tonga-Kermadec)	18–322 km	*Ansell and Gubbins* [1986] and *van der Hilst and Snieder* [1996]
B	—	Japan	—	*Sugioka et al.* [1996]
B	High-f/low-f/several seconds	Tonga	—	*Barazangi et al.* [1972], *Huppert and Frohlich* [1981], and *Ansell and Gubbins* [1986]
B	*S* wave/high-f arrival/~1 min	South America	>500 km	*Isacks and Barazangi* [1973] and *Snoke et al.* [1974]
C	<0.25 Hz/>2 Hz/1–2 s	Northern Japan	185–566 km	*Furumura and Kennett* [2005] and *Furumura and Kennett* [2008]
C	<0.5 Hz/>2 Hz/1–2 s	Western Japan	60–240 km	*Furumura and Kennett* [2008]
C	<0.24 Hz/>2 Hz/~2 s	Indonesian	60–630 km	*Kennett and Furumura* [2008]
C	<1 Hz/>3 Hz/<1 s	Taiwan	60–175 km	This study

source-to-station geometry that allows as less lateral variation of high-velocity layer as possible. Though such high-velocity anomaly layers in the slab develop high-frequency forerunners for propagation over a long distance in the slab, it is very difficult to sustain a large amount of seismic energy within HVL to explain the observation of large and long duration of high-frequency *P* and *S* wave signals.

[29] The type C guided wave has similar characteristics to the type A model with a low-frequency forerunner following large-amplitude and high-frequency *P* and *S* wave coda but is explained by multiple scattering of seismic waves in elongated small-scale heterogeneities inside the slab (named ES) as proposed by *Furumura and Kennett* [2005]. The <0.25 Hz forerunner followed by >2 Hz high-frequency phases with ~2 s separation is commonly found in northern Japan for deeper than 200 km earthquakes where the former oceanic crust no longer keep low-velocity ecologite. Based on finite-difference method modeling of high-frequency seismic wave propagation using a stochastic random heterogeneity plate model, *Furumura and Kennett* [2005] successfully explained the observed characteristics of the slab-guided wave with both the low-frequency forerunner and the following large-amplitude, long-lasting high-frequency *P* and *S* wave energy. In their model, the elongated scatterers in the plate rather than the former oceanic crust (LVL) act to produce the sustained high-frequency coda. Guiding can indeed occur in the former oceanic crust but is delayed relative to the onset of scattered energy. Comparisons of guided wave observations from intra-slab earthquakes in the PSP and Pacific plate in their study suggest that frequency selective wave propagation effect is sensitive to the thickness of the plate and scale lengths of heterogeneity distribution in the plate [*Furumura and Kennett*, 2008]. *Furumura and Kennett* [2008] showed by analysis of dense seismic records and finite-difference simulations that a similar slab-guided wave mechanism is found for intermediate-

depth earthquakes from 60 to 240 km depth in the Nankai-Trough subduction zone where the PSP subducts underneath western Japan. Comparisons of observations of the guided wave from intra-slab earthquakes in the PSP and Pacific plate suggest that the guiding property of the high-frequency signals (e.g., low-frequency and high-frequency separation and frequency of the guided wave, etc.) is very sensitive to the thickness of the heterogeneous plate and the scale lengths of the heterogeneity distribution in the plate [*Furumura and Kennett*, 2008].

[30] The observation of the PSP guided wave in northern Taiwan subduction zone we study here corresponds either to the type A (LVL trapped wave) or type C (scattering in elongated heterogeneities in the plate) or a combination of both effects. Observation in the Taiwan subduction zone of the low-frequency precursor for deeper earthquakes beyond 60 km with large-amplitude high-frequency *P* and *S* wave coda can be explained by the type C guided wave model [*Furumura and Kennett*, 2005, 2008]. However, there are still open questions about how the plate geometry, source-receiver configuration, source location in the plate (e.g., upper or lower planes) influence the observed waveguide behavior in the Taiwan subduction zone and how these different situations play a role in shaping the nature of anomalously large seismic intensity. Resolution of these issues will require more observations coupled to computer simulations for different subduction zone configurations.

7.3. Responsible Structure for Taiwan Guided Waves?

[31] Given the fact that the guided waves events in northern Taiwan and southern Japan occur in the same subducted PSP and exhibit similar high-frequency guiding properties as determined from the spectral ratio of guiding and non-guiding seismograms (see Figures 2e and 2g), the type C guiding provides a suitable model for guided waves observation in this

study. However, it is still possible for the thin waveguide (type A model) to play a role in the guiding phenomenon in northeast Taiwan for earthquakes no deeper than 100 km.

[32] As shown in Table 1, the low-frequency (<1 Hz) first arrival and high-frequency later phases (>3 Hz) observed in the northern Taiwan subduction zone does not show much difference with other areas. However, the time separation between the low- and high-frequency onsets is slightly smaller ($dt < 1$ s) as compared with the guiding behavior from deep focus events in northern Japan. The responsible factors can be either a thinner plate, weaker scattering properties defined by the configuration of the heterogeneity and strength of velocity fluctuation in the PSP slab descending beneath Taiwan. A less bent structure of the PSP slab underneath Taiwan and source-to-receiver geometry may also be a cause of smaller dt [*Furumura and Kennett*, 2005]. The shorter travel distance along the slab in Taiwan leads to less developed high-frequency coda.

[33] By detection and quantification of the subduction zone guided waves, the geometry, thickness, velocity gradient, and heterogeneities of the plates can be further inferred through 2-D and 3-D finite-difference modeling and comparison with other well-established subduction zones. Additionally, knowledge of waveguide characteristics and modeled parameters that fit the observations are critical inputs to connecting with the seismic intensity anomalies for ground motion and earthquake hazard estimation. A demonstration of finite-difference modeling of the scattering waveguide effects will furthermore help us understand the physical nature of subducted slabs underneath Taiwan.

8. Conclusion

[34] Seismic events traveling up subduction zones reveal large-amplitude, high-frequency signal with sustained coda. The character of such guided waves is closely linked to the nature of the subduction zone. The efficiency of propagation of slab-guided waves is a sensitive measure of the present-day plate configuration. Here we have explored different classes of guided waves for the Taiwan-Ryukyu subduction zone earthquakes by analyzing the seismic characteristics of $M > 5$ earthquakes recorded at the CWBSN (Central Weather Bureau Seismic Network) and BATS (Broadband Array in Taiwan for Seismology) stations in Taiwan. Such guided wave behavior is accompanied by anomalous ground shaking levels, which leads to a highly correlated spatial pattern. We found most of the deeper events (>60 km) have dominant frequency at 3–10 Hz, whereas the shallow events (<10 km) show a peak frequency below 3 Hz. The higher-frequency energy is amplified by a factor of 4–400 with longer than 10 -s shaking due to guiding effect, which provides important information for hazard mitigation planning.

[35] A faster arrival of low-frequency signals is visible for all events deeper than 60 km but not for shallower events. This indicates that slab structure is responsible for the differing frequency content between the groups of deeper and shallower events. We find that the time separation of the first motion between low- and high-frequency signals slightly increases with focal depth at some stations, whereas the time separation of the large-amplitude wave trains likely affected by longer travel path in the continental crust increases slightly with propagation distance. In this study, we also obtain a practicable

quantification scheme to determine the duration of higher-frequency energy, which can be regarded as an indicator of the guiding effect of the Philippine Sea Plate.

[36] The situation in Taiwan is one of the few cases in which stations lies on the extension of the subducting plate rather than above it. By comparing with the waveform characteristics produced by numerical simulation of wave propagation models, we argue that this is probably associated with different roles of discrete low-velocity zone and stochastic heterogeneity on trapping high-frequency energy.

References

Abers, G. A. (2000), Hydrated subducted crust at 100–250 km depth, *Earth Planet. Sci. Lett.*, *176*, 323–330.

Abers, G. A., and G. Sarker (1996), Dispersion of regional body waves at 10–150 km depth beneath Alaska: In situ constraints on metamorphism of subducted crust, *Geophys. Res. Lett.*, *23*, 1171–1174.

Abers, G. A., T. Plank, and B. R. Hacker (2003), The wet Nicaraguan slab, *Geophys. Res. Lett.*, *30*(2), 1098, doi:10.1029/2002GL015649.

Ansell, J. H., and D. Gubbins (1986), Anomalous high-frequency wave propagation from the Tonga-Kermadec seismic zone to New Zealand, *Geophys. J. R. Astron. Soc*, *85*, 93–106.

Barazangi, M., B. Isacks, and J. Oliver (1972), Propagation of seismic waves through and beneath the lithosphere that descends under the Tonga Island Arc, *J. Geophys. Res.*, *77*, 952–958.

Biq, C. C. (1973), Kinematic pattern of Taiwan as an example of actual continent-arc collision, *Report of the Seminar on Seismology, US-ROC Cooperative Science Program*, 21–26.

Bowin, C., R. Lu, C. S. Lee, and H. Chouten (1978), Plate convergence and accretion in Taiwan-Luzon region, *Am. Assoc. Pet. Geol. Bull.*, *62*, 1645–1672.

Chang, Y. F., and B. S. Huang (2002), A study of early high-frequency precursors by physical modeling, *Terr. Atmos. Oceanic Sci.*, *13*(1), 1–14.

Chen, P. F., B. S. Huang, and L. Y. Chiao (2011), Upper mantle seismic velocity anomaly beneath southern Taiwan as revealed by teleseismic relative arrival times, *Tectonophysics*, *498* (1-4), 27–34.

Chen, P. F., B. S. Huang, and W. T. Liang (2004), Evidence of a slab of subducted lithosphere beneath central Taiwan from seismic waveforms and travel times, *Earth Planet. Sci. Lett.*, *229*, 61–71.

Chen, P. F., C. R. Bina, H. Kuo-Chen, F. T. Wu, C. Y. Wang, B. S. Huang, C. H. Chen, and W. T. Liang (2012), Slab-induced waveform effects as revealed by the TAIGER seismic array: Evidence of slab beneath central Taiwan, *Earth Planet. Sci. Lett.*, http://dx.doi.org/10.1016/j.pepi.2012.02.004.

Chiu, J. M., B. L. Isacks, and R. K. Cardwell (1985), Propagation of high-frequency seismic waves inside the subducted lithosphere from intermediate-depth earthquakes recorded in the Vanuatu, *J. Geophys. Res.*, *90*, 12,741–12,754.

Chou, H. C., B. Y. Kuo, S. H. Hung, L. Y. Chiao, D. Zhao, and Y. M. Wu (2006), The Taiwan-Ryukyu subduction-collision complex: Folding of a viscoelastic slab and the double seismic zone, *J. Geophys. Res.*, *111*, B04410, doi:10.1029/2005JB003822.

Essen, K., M. Braatz, L. Ceranna, W. Friederich, and T. Meier (2009), Numerical modeling of seismic wave propagation along the plate contact of the Hellenic subduction zone the influence of a deep subduction channel, *Geophys. J. Int.*, *179*, 1737–1756.

Fukao, Y., S. Hori, and M. Ukawa (1983), A seismological constraining on the depth of basalt-ecologite transition in a subducting oceanic crust, *Nature*, *303*, 413–415.

Furumura, T., and B. L. N. Kennett (2005), Subduction zone guided waves and the heterogeneity structure of the subducted plate—Intensity anomalies in northern Japan, *J. Geophys. Res.*, *110*, B10302, doi:10.129/2004JB003486.

Furumura, T., and B. L. N. Kennett (2008), A scattering waveguide in the heterogeneous subducting plate, in: Dmowska, R. (Ed.), Earth Heterogeneity and Scattering Effects on Seismic Waves, *Adv. Geophys.*, *50*, 195–217.

Galea, P. (1992), Observations of very high P-velocities in the subducted slab, New Zealand, and their relation with the slab geometry, *Geophys. J. Int.*, *110*, 238–250.

Gubbins, D., and R. Snieder (1991), Dispersion of P waves in subducted lithosphere: Evidence for an ecoglite layer, *J. Geophys. Res.*, *96*, 6321–6333.

Gubbins, D., J. Barnicoat, and J. Cann (1994), Seismological constraints on the gabbro-eclogite-eclogite transition in subducted oceanic crust, *Earth Planet. Sci. Lett.*, *122*, 89–101.

Hasegawa, K. (1918), An earthquake under the Sea of Japan, *J. Meteorol. Soc. Jpn.*, *37*, 203–207.

Ho, C. S. (1986), A synthesis of the geologic evolution of Taiwan, *Tectonophysics*, *125*, 1–16.

Hori, S., H. Inoue, Y. Fukao, and M. Ukawa (1985), Seismic detection of the untransformed "basaltic" oceanic crust subducting into the mantle, *Geophys. J. R. Astron. Soc.*, *83*, 169–197.

Huppert, L. N., and C. Frohlich (1981), The P wave velocity within the Tonga Benioff Zone determined from traced rays and observations, *J. Geophys. Res.*, *86*, 3771–3782.

Isacks, B. L., and M. Barazangi (1973), High-frequency shear waves guided by a continuous lithosphere descending beneath western South America, *Geophys. J. R. astr. Soc.*, *33*, 129–139.

Ishikawa, T. (1926), On seismograms of earthquakes exhibiting abnormal distribution of seismic intensities, *Q. J. Seismol.*, *2*, 7–15.

Kao, H., S. J. Shen, and K. F. Ma (1998), Transition from oblique subduction to collision: Earthquakes in the southernmost Ryukyu arc—Taiwan region, *J. Geophys. Res.*, *103*, 7211–7299.

Kawakatsu, H., and S. Watada (2007), Seismic evidence for deep water transportation in the mantle, *Science*, *316*, 1468–1471.

Kennett B. L. N., and T. Furumura (2008), Stochastic waveguide in the lithosphere: Indonesian subduction zone to Australian craton, *Geophys. J. Int.*, *172*, 363–382.

Kita, S., T. Okada, J. Nakajima, T. Matsuzawa, and A. Hasegawa (2006), Existence of a seismic belt in the upper plane of the double seismic zone extending in the along-arc direction at depths of 70–100 km beneath NE Japan, *Geophys. Res. Lett.*, *33*, doi:10.1029/2006GL028239.

Konstantinou, K. I., and N. S. Melis (2008), High-requency shear-wave propagation across the Hellenic subduction zone, *Bull. Seismol. Soc. Am.*, *98*(2), 797–803, doi:10.1785/0120060238.

Lee, C. T., C. T. Cheng, C. W. Liao, and Y. B. Tsai (2001), Site classification of Taiwan free-field strong-motion stations, *Bull. Seismol. Soc. Am.*, *91*(5), 1283–1297.

Lin, C. H. (2002), Active continental subduction and crustal exhumation: The Taiwan Orogeny, *Terra Nova*, *14*, 281–287.

Lin, C. H. (2009), Compelling evidence of an aseismic slab beneath central Taiwan from a dense linear seismic array, *Tectonophysics*, *466*, 205–212.

Lallemand, S., Y. Font, H. Bijwaard, and H. Kao (2001), New insights on 3-D plates interaction near Taiwan from tomography and tectonic implications, *Tectonophysics*, *335*, 229–253.

Lallemand, S. E., C. S. Liu, and Y. Font (1997), A tear fault boundary between the Taiwan orogeny and the Ryukyu subduction zone, *Tectonophysics*, *274*(1–3), 171–190.

Martin, S., and A. Rietbrock (2006), Guided waves at subduction zones: Dependencies on slab geometry receiver locations and earthquake sources, *Geophys. J. Int.*, *167*, 693–704.

Martin, S., A. Rietbrock, C. Haberland, and G. Asch (2003), Guided waves propagating in subducted oceanic crust, *J. Geophys. Res.*, *108*(B11), 2536, doi:10.1029/2003JB002450.

Oda, H., T. Tanaka, and K. Seya (1990), Subducting oceanic crust on the Philippine Sea Plate in southwest Japan, *Tectonophysics*, *172*, 175–189.

Seno, T. (1977), The instantaneous rotation vector of the Philippine Sea Plate relative to the Eurasian plate, *Tectonophysics*, *42*, 209–226.

Seno, T., S. Stein, and A. E. Gripp (1993), A model for the motion of the Phillippine Sea plate consistent with NUVEL-1 and geologic data, *J. Geophys. Res.*, *98*, 17941–17948.

Shin, T. C. (1992), Some implications of Taiwan tectonic features from the data collected by the Central Weather Bureau Seismic Network, *Meteorol. Bull.*, *38*, 23–48.

Smith, G. P., D. Gubbins, and W. Mao (1994), Fast P waves propagation in subducted Pacific lithosphere: Refraction from the plate, *J. Geophys. Res.*, *99*, 23,787–23,800.

Snoke, J. A., I. S. Sacks, and H. Okada (1974), A model not requiring continuous lithosphere for anomalous high-frequency arrivals from deep-focus South American earthquakes, *Phys. Earth Planet. Inter.*, *9*, 199–206.

Stuart, G. W., D. Francis, D. Gubbins, and G. Smith (1995), Tararua broadband array, North Island, New Zealand, *Bull. Seismol. Soc. Am.*, *85*, 325–333.

Sugioka, H., Fukao, Y., and Sakai, S. (1996), Anomalously early first arrivals to the J-array from teleseismic events, *J. Phys. Earth*, *44*, 687–699.

Suppe, J., J. G. Liou, and W. G. Ernst (1981), Paleogeographic origins of the Miocene East Taiwan Ophiolite, *Am. J. Sci.*, *281*, 228–246.

Tsuji, Y., J. Nakajima, and A. Hasegawa (2008), Tomographic evidence for hydrated oceanic crust of the Pacific slab beneath northeastern Japan: Implications for water transportation in subduction zones, *Geophys. Res. Lett.*, *35*, L14308, doi:10.1029/2008GL034461.

Ustaszewski, K., Y. M. Wu, J. Suppe, H. H. Huang, C. H. Chang, and S. Carena (2012), Crust-mantle boundaries in the Taiwan-Luzon arc-continent collision system determined from local earthquake tomography and 1D models: Implications for the mode of subduction polarity reversal, Tectonophysics, *Special Issue: Geodyn. Environ. East. Asia.*, *578*, 31–49, doi:10.1016/j.tecto.2011.12.029.

Utsu, T. (1966), Regional difference in absorption of seismic waves in the upper mantle as inferred from abnormal distribution of seismic intensities, *J. Fac. Sci. Hokkaido Univ., Ser. VII*, *2*, 359–374.

Utsu, T., and H. Okada (1968), Anomalies in seismic wave velocity and attenuation associated with a deep earthquake zone (II), *J. Fac. Sci. Hokkaido Univ., Ser. VII*, *3*, 65–84.

van der Hilst, R., and R. Snieder (1996), High-frequency precursors to P waves arrivals in New Zealand: Implications for slab structure, *J. Geophys. Res.*, *101*, 8473–8488.

Wang, Z., D. Zhao, J. Wang, and H. Kao (2006), Tomographic evidence for the Eurasian lithosphere subducting beneath south Taiwan, *Geophys. Res. Lett.*, *33*, L18306. doi:10.1029/2006GL027166.

Wang, Z., Y. Fukao, D. Zhao, S. Kodaira, O. P. Mishra, and A. Yamada (2009), Structural heterogeneities in the crust and upper mantle beneath Taiwan, *Tectonophysics*, *476*,460–477.

Wu, F. T., R. J. Rau, and D. Salzberg (1997), Taiwan orogeny: Thin-skinned or lithospheric collision?, *Tectonophysics*, *274*, 191–220.

Wu, F.T., W. T. Liang, J. C. Lee, H. Benz, and A. Villasenor (2009), A model for the termination of the Ryukyu subduction zone against Taiwan: A junction of collision, subduction/separation, and subduction boundaries, *J. Geophys. Res.*, *114*, B07404, doi:10.1029/2008JB005950.

Wu, Y. M., C. H. Chang, L. Zhao, J. B. H. Shyu, Y. G. Chen, K. Sieh, and J. P. Avouac (2007), Seismic tomography of Taiwan: Improved constraints from a dense network of strong motion stations, *J. Geophys. Res.*, *112*, B08312, doi:10.1029/2007JB004983.

Yu, S. B., H. Y. Chen, and L. C. Kuo (1977), Velocity field of GPS stations in the Taiwan area, *Tectonophysics*, *274*, 41–59.